

CHAPTER FOUR

Investigation of absorption-dispersion relation without dipole-dipole interaction (off resonance case)

4.1 Introduction

We proceed our investigation of the absorption-dispersion relation from two collective atoms damped by a normal vacuum without the inclusion of dipole-dipole interaction and driven by a detuned laser. Our aim is to study the absorption-dispersion profile with finite detunings and without dipole-dipole interaction. We intend to know how the spectrum looks like in comparison with the corresponding zero detuning case with dipole-dipole interaction as done in previous chapter. The motivation is to achieve finite dispersion accompanied by zero absorption.

The formal apparatus used here is the secular approximation technique which has been applied with considerable success to a variety of atom-field interaction problems. The technique was first introduced by Agarwal et al [4.1] to a system of N atoms with zero detuning and driven by a strong monochromatic driving field. Later, the method has been generalised with non-zero detuning in the two atoms system [4.2-4.6]. The fact that they were restricted only to two atoms system was due to a difficulty in

obtaining a closed set of equations when a detuning is present. In 1985, Lawande et al [4.7] made a further generalisation by including phase and amplitude fluctuations of the strong driving field and also take into account dipole-dipole interactions. This generalisation has a limitation because it is only valid in the regime of small dipole interactions. Later Cordes [4.8] made another improvement by extending the secular approximation technique that includes dipole-dipole interaction coupling comparable in strength with the Rabi frequency. Now, the new 'slowly varying' operators are no longer simply a rotation of the original collective operators, but rather involve the complete set of eight atomic operators for the two atoms system. In this generalisation, it is crucial to include the full undamped Hamiltonian H_0 in carrying out the transformation to a set of slowly varying operators. The failure to include the complete H_0 in the transformation leads to a limited form of secular approximation with a restricted range of validity. Cordes analysis was carried out only for the case of zero detuning. To extend for non-zero detuning, more effort is required as the calculation will be much more complicated particularly in both the decoupling and solving of the operator differential equations for \bar{S}^x and \bar{S}^y and in the succeeding stages of the calculation. By simplifying the technique i.e. ignoring dipole-dipole interactions, we observe that the absorption spectra vanish for zero detuning unless one goes beyond the lowest order of the secular approximation [4.6]. Hence, we use a secular approximation technique only for the case of non-zero detuning and not taking into account dipole-dipole interactions between the atoms. So, the cooperative behaviour stems entirely from the mutual coupling of the two atoms with the strong coherent driving field.

4.2 Master equation without dipole-dipole interactions

The particular master equation describing the evolution of a system of two closely spaced two-level atoms in a rotating frame at frequency ω_L (the laser frequency) is [4.4]:

$$\frac{\partial \rho}{\partial t} = -i[H_0, \rho] - \gamma(S^+ S^- \rho + \rho S^+ S^- - 2S^- \rho S^+) \quad (4.2.1)$$

where 2γ is the Einstein A coefficient, S^+ and S^- are the usual collective atomic dipole operators and ρ is the reduced atomic density operator. H_0 is the Hamiltonian describing the coupling of the atoms to an external coherent driving field of frequency ω_L :

$$H_0 = -\Omega(S^+ + S^-) - \Delta S^z = -2\Omega S^x - \Delta S^z \quad (4.2.2)$$

2Ω is the Rabi frequency, $\Delta = \omega_L - \omega_0$ is the detuning of the laser from the atomic resonance and $S^z = \frac{1}{2}[S^+, S^-]$. For high field strengths, $\Omega \gg 2\gamma$, an approximation first introduced by Cordes [4.4] can be used to simplify the master equation (4.2.1).

Consider the new operators

$$\bar{S}^i(t) = V(t)S^iV^{-1}(t) \quad i = 1, 2, 3 \quad (4.2.3)$$

where

$$S^1 = S^x \quad S^2 = S^y \quad S^3 = S^z \quad (4.2.4)$$

$$V(t) = \exp(-iH_0 t) \quad (4.2.5)$$

The transformed operators $\bar{S}^i(t)$ have the property that their expectation values are slowly varying. In particular, we have the equation of motion for $\langle t | \bar{S}^i(t) | t \rangle$ (in Schrödinger picture with the states $|t\rangle$)

$$\begin{aligned} \frac{d}{dt} \langle t | \bar{S}^i(t) | t \rangle &= \text{Tr} \bar{S}^i \frac{\partial \rho}{\partial t} + \left\langle t \left| \frac{\partial \bar{S}^i}{\partial t} \right| t \right\rangle \\ &= -\gamma \text{Tr} \bar{S}^i (S^+ S^- \rho + \rho S^+ S^- - 2S^- \rho S^+) \end{aligned} \quad (4.2.6)$$

The idea underlying the approximation technique is to evaluate the \bar{S}^i using equation (4.2.3), express S^i in terms of \bar{S}^i , and then replace S^\pm in the master equation (4.2.1). As a result certain terms are slowly varying while others are rapidly oscillating. The secular approximation then consists of dropping these rapidly oscillating terms. Using equations (4.2.2)-(4.2.4) we eventually get

$$\bar{S}^x = \frac{4\Omega + \Delta^2 \cos \alpha t}{\alpha^2} S^x - \left(\frac{\Delta}{\alpha} \sin \alpha t \right) S^y + \frac{2\Delta\Omega}{\alpha^2} (1 - \cos \alpha t) S^z$$

$$\bar{S}^y = \left(\frac{\Delta}{\alpha} \sin \alpha t\right) S^x + (\cos \alpha t) S^y - \left(\frac{2\Omega}{\alpha} \sin \alpha t\right) S^z \quad (4.2.7)$$

$$\bar{S}^z = \frac{2\Delta\Omega}{\alpha^2} (1 - \cos \alpha t) S^x + \left(\frac{2\Omega}{\alpha} \sin \alpha t\right) S^y + \frac{\Delta^2 + 4\Omega \cos \alpha t}{\alpha^2} S^z$$

where $\alpha = (4\Omega^2 + \Delta^2)^{1/2}$ is the generalised Rabi frequency. Further, using

$S^\pm = S^x \pm iS^y$ we get

$$S^+ = \frac{i}{2} \left(1 + \frac{\Delta}{\alpha}\right) R^+ + \frac{i}{2} \left(1 - \frac{\Delta}{\alpha}\right) R^- + \frac{2\Omega}{\alpha} R^z$$

$$S^- = \frac{i}{2} \left(1 - \frac{\Delta}{\alpha}\right) R^+ - \frac{i}{2} \left(1 + \frac{\Delta}{\alpha}\right) R^- + \frac{2\Omega}{\alpha} R^z$$

$$S^z = -\frac{i\Omega}{\alpha} R^+ + \frac{i\Omega}{\alpha} R^- + \frac{\Omega}{\alpha} R^z$$

(4.2.8)

where

$$R^+ = \left(-\frac{i\Delta}{\alpha} \bar{S}^x + \bar{S}^y + \frac{2i\Omega}{\alpha} \bar{S}^z\right) e^{-i\alpha t}$$

$$R^- = \left(\frac{i\Delta}{\alpha} \bar{S}^x + \bar{S}^y - \frac{2i\Omega}{\alpha} \bar{S}^z\right) e^{i\alpha t}$$

$$R^z = \left(\frac{2\Omega}{\alpha} \bar{S}^x + \frac{\Delta}{\alpha} \bar{S}^z\right)$$

(4.2.9)

It then follows from equations (4.2.7) and (4.2.9) that

$$\begin{aligned}
 R^x &= \frac{1}{2}(R^+ + R^-) = S^y \\
 R^y &= \frac{(R^+ - R^-)}{2i} = -\frac{\Delta}{\alpha}S^x + \frac{2\Omega}{\alpha}S^z \\
 R^z &= \frac{2\Omega}{\alpha}S^x + \frac{\Delta}{\alpha}S^z
 \end{aligned}
 \tag{4.2.10}$$

The R operators (R^x, R^y, R^z) being a rotation of the S operators obey the usual angular momentum commutation relations. For intense fields, the operators R^\pm vary with time approximately as $\exp(\mp i\alpha t)$, while R^z is a slowly varying operator. From equation (4.2.1) and using equation (4.2.8) and also dropping rapidly oscillating terms such as R^+R^z, R^+R^+ , etc. we find an approximate master equation of the form

$$\begin{aligned}
 \frac{\partial \rho}{\partial t} &= i\alpha[R^z, \rho] - \gamma\{(1-r)(R^zR^z\rho + \rho R^zR^z - 2R^z\rho R^z) \\
 &\quad + \frac{1}{4}\left(1 + \frac{\Delta}{\alpha}\right)^2 (R^+R^-\rho + \rho R^+R^- - 2R^- \rho R^+) \\
 &\quad + \frac{1}{4}\left(1 - \frac{\Delta}{\alpha}\right)^2 (R^-R^+\rho + \rho R^-R^+ - 2R^+ \rho R^-)\}
 \end{aligned}
 \tag{4.2.11}$$

where $r = \left(\frac{\Delta}{\alpha}\right)^2$. The equation of motion for the expectation value of an arbitrary operator O follows from (4.2.11):

$$\begin{aligned}
\langle \dot{O} \rangle &= i\alpha \langle [O, R^z] \rangle - \gamma \{ (1-r) \langle [[O, R^z], R^z] \rangle \\
&+ \frac{1}{4} (1+r) \langle [[O, R^+], R^-] \rangle + \langle [[O, R^-], R^+] \rangle \rangle \\
&+ \frac{1}{2} \Delta \alpha^{-1} \langle ([O, R^+], R^- \rangle - \langle [[O, R^-], R^+] \rangle \rangle \} \quad (4.2.12)
\end{aligned}$$

where anti commutator $[A, B]_- = AB + BA$. Further, we now introduce the additional operators

$$\begin{aligned}
L &= R^z R^+ + R^+ R^z & L^* &= R^z R^- + R^- R^z \\
N &= R^+ R^- + R^- R^+ & A &= R^+ R^+ & B &= R^- R^- \quad (4.2.13)
\end{aligned}$$

The eight operators R^+ , R^- , R^z , L , L^* , N , A and B with their identity form a complete set of independent atomic operators in the triplet subspace of a two atoms system. Using (4.2.12) and (4.2.13), we get the equations of motion for the transformed operators

$$\langle \dot{R}^+ \rangle = \left[-i\alpha - \frac{3}{2} \gamma \left(1 - \frac{1}{3} r \right) \right] \langle R^+ \rangle + \frac{\Delta}{\alpha} \gamma \langle L \rangle$$

$$\langle \dot{R}^z \rangle = -\gamma (1+r) \langle R^z \rangle - \frac{\Delta}{\alpha} \gamma \langle N \rangle$$

$$\langle \dot{L} \rangle = \left[-i\alpha - \frac{7}{2} \gamma \left(1 + \frac{3}{7} r \right) \right] \langle L \rangle - 3\gamma \frac{\Delta}{\alpha} \langle R^+ \rangle$$

$$\langle \dot{N} \rangle = -3\gamma(1+r)\langle N \rangle + 4\gamma \frac{\Delta}{\alpha} \langle R^z \rangle + 8\gamma(1+r)$$

$$\langle \dot{A} \rangle = [-2i\alpha - \gamma(5-3r)]\langle A \rangle$$

$$\langle \dot{B} \rangle = [2i\alpha - \gamma(5-3r)]\langle B \rangle$$

(4.2.14)

Equations for $\langle \dot{R}^+ \rangle$ and $\langle \dot{L} \rangle$ form a coupled pair, as do equations for $\langle \dot{R}^z \rangle$ and $\langle \dot{N} \rangle$. In a two atoms system, at most two quantities get coupled together when the R variables are used. For example, consider equation (4.2.9). It is known that $\langle R^+ \rangle$ has the characteristic time dependence $\exp(-i\alpha t)$ while $\langle R^- \rangle$ depends on $\exp(i\alpha t)$ and $\langle R^z \rangle$ is constant. Therefore, in addition to $\langle R^+ \rangle$, only $\langle L \rangle$ could possibly enter the equation of motion for $\langle R^+ \rangle$ and conversely. Similar arguments apply to $\langle R^z \rangle$ and $\langle N \rangle$. Imposing Laplace transforms on the equations for $\langle \dot{R}^+ \rangle$ and $\langle \dot{L} \rangle$ and eliminating $\langle L \rangle$ result in the following:

$$\langle \tilde{L} \rangle = \frac{1}{f_+(s)} \left\{ \left[s + i\alpha + \frac{3\gamma}{2} \left(1 - \frac{r}{3} \right) \right] \langle L(0) \rangle - 3\Delta\alpha^{-1}\gamma \langle R^+(0) \rangle \right\} \quad (4.2.15)$$

$$\langle \tilde{L}^+ \rangle = \frac{1}{f_-(s)} \left\{ \left[s - i\alpha + \frac{3\gamma}{2} \right] \left(1 - \frac{r}{3} \right) \langle L^+(0) \rangle - 3\Delta\alpha^{-1}\gamma \langle R^-(0) \rangle \right\} \quad (4.2.16)$$

$$\langle \tilde{R}^+ \rangle = \frac{1}{f_+(s)} \left\{ \left[s + i\alpha + \frac{7\gamma}{2} \left(1 + \frac{3r}{7} \right) \right] \langle R^+(0) \rangle + \Delta\alpha^{-1}\gamma \langle L(0) \rangle \right\} \quad (4.2.17)$$

$$\langle \bar{R}^- \rangle = \frac{1}{f_-(s)} \left\{ \left[s - i\alpha + \frac{7\gamma}{2} \left(1 + \frac{3r}{7} \right) \right] \langle R^-(0) \rangle + \Delta\alpha^- \gamma \langle L^+(0) \rangle \right\} \quad (4.2.18)$$

where

$$f_-(s) = (s + i\alpha + \gamma_3)(s + i\alpha + \gamma_4)$$

$$f_+(s) = (s - i\alpha + \gamma_3)(s - i\alpha + \gamma_4)$$

$$\gamma_3 = \gamma \left[\frac{1}{2}(5+r) - \sqrt{1-r+r^2} \right]$$

$$\gamma_4 = \gamma \left[\frac{1}{2}(5+r) + \sqrt{1-r+r^2} \right]$$

(4.2.19)

Note that now s is the Laplace transform variable. Also from the equations for $\langle \bar{R}^z \rangle$

and $\langle \bar{N} \rangle$ in equation (4.2.14) we obtain

$$\langle \bar{R}^z \rangle = \frac{1}{f_z(s)} \left\{ [s + 3\gamma(1+r)] \langle R^z(0) \rangle - \frac{\Delta\gamma}{\alpha} \langle N(0) \rangle - \frac{8\Delta\gamma^2}{s\alpha} (1+r) \right\} \quad (4.2.20)$$

$$\langle \bar{N} \rangle = \frac{1}{f_z(s)} \left\{ [s + \gamma(1+r)] \langle N(0) \rangle + \frac{4\Delta\gamma}{\alpha} \langle R^z(0) \rangle + 8\gamma(1+r) + \frac{8\gamma^2(1+r)^2}{s} \right\} \quad (4.2.21)$$

where

$$f_z(s) = (s + \gamma_1)(s + \gamma_2)$$

$$\gamma_1 = \gamma(1+3r)$$

$$\gamma_2 = \gamma(3+r)$$

(4.2.22)

Finally, from equations for $\langle \tilde{A} \rangle$ and $\langle \tilde{B} \rangle$ in equation (4.2.14) we get via Laplace transformation:

$$\langle \tilde{A} \rangle = \frac{1}{s + 2i\alpha + \gamma(5 - 3r)} \langle A(0) \rangle \quad (4.2.23)$$

$$\langle \tilde{B} \rangle = \frac{1}{s - 2i\alpha + \gamma(5 - 3r)} \langle B(0) \rangle \quad (4.2.24)$$

Combining equations (4.2.8), (4.2.17), (4.2.18) and (4.2.20) and using the quantum regression theorem [4.9] yields the Laplace transform of the two - time atomic correlation function:

$$\begin{aligned} \overline{\langle \tilde{S}^+(t+\tau) \tilde{S}^-(\tau) \rangle}_{ss} &= \int_0^\infty d\tau \exp(-s\tau) \langle S^+(t+\tau) S^-(\tau) \rangle_{ss} \\ &= \frac{i}{2f_+(s)} \left(1 + \frac{\Delta}{\alpha}\right) \left\{ \left[s + i\alpha + \frac{7\gamma}{2} \left(1 + \frac{3r}{7}\right) \right] \langle R^+ S^- \rangle_{ss} + \Delta \alpha^{-1} \gamma \langle LS^- \rangle_{ss} \right\} \\ &+ \frac{i}{2f_-(s)} \left(1 - \frac{\Delta}{\alpha}\right) \left\{ \left[s - i\alpha + \frac{7\gamma}{2} \left(1 + \frac{3r}{7}\right) \right] \langle R^- S^- \rangle_{ss} + \Delta \alpha^{-1} \gamma \langle L^+ S^- \rangle_{ss} \right\} \\ &+ \frac{2\Omega}{\alpha f_z(s)} \left\{ [s + 3\gamma(1+r)] \langle R^+ S^- \rangle_{ss} - \Delta \alpha^{-1} \gamma \langle NS^- \rangle_{ss} - \frac{8\gamma^2 \Delta \alpha^{-1}}{s} (1+r) \langle S^- \rangle_{ss} \right\} \end{aligned} \quad (4.2.25)$$

Similarly ,

$$\begin{aligned}
\overbrace{\langle \tilde{S}^-(\tau) \tilde{S}^+(t+\tau) \rangle_{ss}} &= \int_0^\infty d\tau \exp(-s\tau) \langle S^-(\tau) S^+(t+\tau) \rangle_{ss} \\
&= \frac{i}{2f_-(s)} \left(1 + \frac{\Delta}{\alpha}\right) \left\{ \left[s + i\alpha + \frac{7\gamma}{2} \left(1 + \frac{3r}{7}\right) \right] \langle S^- R^+ \rangle_{ss} + \Delta \alpha^{-1} \gamma \langle S^- L \rangle_{ss} \right\} \\
&+ \frac{i}{2f_-(s)} \left(1 - \frac{\Delta}{\alpha}\right) \left\{ \left[s - i\alpha + \frac{7\gamma}{2} \left(1 + \frac{3r}{7}\right) \right] \langle S^- R^- \rangle_{ss} + \Delta \alpha^{-1} \gamma \langle S^- L^+ \rangle_{ss} \right\} \\
&+ \frac{2\Omega}{\alpha f_z(s)} \left\{ [s + 3\gamma(1+r)] \langle S^- R^z \rangle_{ss} - \Delta \alpha^{-1} \gamma \langle S^- N \rangle_{ss} - \frac{8\gamma^2 \Delta \alpha^{-1}}{s} (1+r) \langle S^- \rangle_{ss} \right\}
\end{aligned} \tag{4.2.26}$$

The steady-state expectation values in equations (4.2.25) and (4.2.26) can be evaluated by expressing all the products of the operators entirely in terms of the R operators and results in the following :

$$\begin{aligned}
\langle R^\pm \rangle_{ss} &= \langle L \rangle_{ss} = \langle L^+ \rangle_{ss} = \langle A \rangle_{ss} = \langle B \rangle_{ss} = 0 \\
\langle R^z \rangle_{ss} &= -2\Delta \alpha^3 D^{-1} (1+r) \\
\langle N \rangle_{ss} &= 2\Delta \alpha^4 D^{-1} (1+r)^2 \\
\langle R^+ S^- \rangle_{ss} &= -\frac{i\alpha^4 D^{-1}}{2} \left(1 - \frac{\Delta}{\alpha}\right) (1-r^2) \\
\langle R^- S^- \rangle_{ss} &= -\frac{i\alpha^4 D^{-1}}{2} \left(1 + \frac{\Delta}{\alpha}\right) (1-r^2) \\
\langle R^z S^- \rangle_{ss} &= \langle S^- R^z \rangle_{ss} = \Omega \alpha^3 D^{-1} (1+6r+r^2)
\end{aligned}$$

$$\begin{aligned}
\langle S^-R^+ \rangle_{ss} &= \frac{i\alpha^4 D^{-1}}{2} \left\{ \left(1 - \frac{\Delta}{\alpha} \right) (1-r) - 4 \left(r + \frac{\Delta}{\alpha} \right) \right\} (1+r) \\
\langle S^-R^- \rangle_{ss} &= \frac{i\alpha^4 D^{-1}}{2} \left\{ \left(1 + \frac{\Delta}{\alpha} \right) (1-r) - 4 \left(\frac{\Delta}{\alpha} - r \right) \right\} (1+r) \\
\langle S^-L \rangle_{ss} &= -i \left\{ \frac{1}{2} \left(1 + \frac{\Delta}{\alpha} \right) [6\alpha^4 D^{-1} (1+r)^2 - 8] + \Delta \alpha^3 D^{-1} \left(1 - \frac{\Delta}{\alpha} \right) (1-r) \right\} \\
\langle S^-L^+ \rangle_{ss} &= -i \left\{ \frac{1}{2} \left(1 - \frac{\Delta}{\alpha} \right) [6\alpha^4 D^{-1} (1+r)^2 - 8] + \Delta \alpha^3 D^{-1} \left(1 + \frac{\Delta}{\alpha} \right) (1-r) \right\} \\
\langle LS^- \rangle_{ss} &= i\Delta \alpha^3 D^{-1} \left(1 - \frac{\Delta}{\alpha} \right) (1-r) \\
\langle L^+S^- \rangle_{ss} &= i\Delta \alpha^3 D^{-1} \left(1 + \frac{\Delta}{\alpha} \right) (1-r) \\
\langle NS^- \rangle_{ss} &= \langle S^-N \rangle_{ss} = -8\Delta \Omega \alpha^2 D^{-1} (1+r)
\end{aligned}
\tag{4.2.27}$$

where

$$D = \frac{\alpha^4 (1+3r)(3+r)}{4}.$$

Note: There are two printing errors occurred on some of the expressions in equation (4.2.27) in ref[4.4].

4.3 Absorption and dispersion spectrum

The steady-state absorption spectrum in the rotating frame is defined by the Fourier transform (see e.g Cordes and Chevary (1984) [4.6]) :

$$R(\omega) = \text{Re} \int_0^{\infty} d\tau \exp(-s\tau) \lim_{t \rightarrow \infty} \langle [S^-(\tau), S^+(\tau+t)] \rangle \quad (4.3.1)$$

From equations (4.2.25), (4.2.26) and (4.3.1), we thus get:

$$R(\omega) = \text{Re} \left\{ \frac{i}{2f_+(s)} \left(1 + \frac{\Delta}{\alpha} \right) \left[\left[s + i\alpha + \frac{7\gamma}{2} \left(1 + \frac{3r}{7} \right) \right] \langle [S^-, R^+] \rangle_{ss} + \Delta \alpha^{-1} \gamma \langle [S^-, L] \rangle_{ss} \right] \right. \\ \left. + \frac{i}{2f_-(s)} \left(1 - \frac{\Delta}{\alpha} \right) \left[\left[s - i\alpha + \frac{7\gamma}{2} \left(1 + \frac{3r}{7} \right) \right] \langle [S^-, R^-] \rangle_{ss} + \Delta \alpha^{-1} \gamma \langle [S^-, L^+] \rangle_{ss} \right] \right\}_{s=i(\omega-\omega_L)} \quad (4.3.2)$$

The commutators $[S^-, R^+]$, $[S^-, L]$, $[S^-, R^-]$ and $[S^-, L^+]$ can be calculated using equation (4.2.8) and are

$$\langle [S^-, R^+] \rangle_{ss} = -2i\Delta\alpha^3 D^{-1} \left(1 + \frac{\Delta}{\alpha} \right) (1+r) \\ \langle [S^-, R^-] \rangle_{ss} = -2i\Delta\alpha^3 D^{-1} \left(1 - \frac{\Delta}{\alpha} \right) (1+r) \\ \langle [S^-, L^+] \rangle_{ss} = -\frac{i}{2} \left(1 - \frac{\Delta}{\alpha} \right) (8 - 6\alpha^4 D^{-1} (1+r)^2) \\ \langle [S^-, L] \rangle_{ss} = -\frac{i}{2} \left(1 + \frac{\Delta}{\alpha} \right) (6\alpha^4 D^{-1} (1+r)^2 - 8) \quad (4.3.3)$$

Finally, we get our approximation for the two-atom absorption spectrum:

$$\begin{aligned}
 R(\omega) = & \operatorname{Re} \left[\frac{\Delta}{2f_+(s)} \left(1 + \frac{\Delta}{\alpha} \right)^2 \left\{ \left[s + i\alpha + \frac{7\gamma}{2} \left(1 + \frac{3r}{7} \right) \right] \frac{2}{D} \alpha^3 (1+r) - \frac{\gamma}{2\alpha} \left(\frac{6}{D} \alpha^4 (1+r)^2 - 8 \right) \right\} \right. \\
 & \left. - \frac{\Delta}{2f_-(s)} \left(1 - \frac{\Delta}{\alpha} \right)^2 \left\{ \left[s - i\alpha + \frac{7\gamma}{2} \left(1 + \frac{3r}{7} \right) \right] \frac{2}{D} \alpha^3 (1+r) - \frac{\gamma}{2\alpha} \left(8 - \frac{6}{D} \alpha^4 (1+r)^2 \right) \right\} \right]_{s=i(\omega-\omega_L)}
 \end{aligned}
 \tag{4.3.4}$$

For the dispersion spectra, it is represented by corresponding the imaginary part of complex Fourier transform see e.g.[4.10]:

$$\begin{aligned}
 \chi(\omega) = & \operatorname{Im} \int_0^{\infty} d\tau \exp(-s\tau) \lim_{t \rightarrow \infty} \langle [S^-(\tau), S^+(\tau+t)] \rangle \\
 = & \operatorname{Im} \left[\frac{\Delta}{2f_+(s)} \left(1 + \frac{\Delta}{\alpha} \right)^2 \left\{ \left[s + i\alpha + \frac{7\gamma}{2} \left(1 + \frac{3r}{7} \right) \right] \frac{2}{D} \alpha^3 (1+r) - \frac{\gamma}{2\alpha} \left(\frac{6}{D} \alpha^4 (1+r)^2 - 8 \right) \right\} \right. \\
 & \left. - \frac{\Delta}{2f_-(s)} \left(1 - \frac{\Delta}{\alpha} \right)^2 \left\{ \left[s - i\alpha + \frac{7\gamma}{2} \left(1 + \frac{3r}{7} \right) \right] \frac{2}{D} \alpha^3 (1+r) - \frac{\gamma}{2\alpha} \left(8 - \frac{6}{D} \alpha^4 (1+r)^2 \right) \right\} \right]_{s=i(\omega-\omega_L)}
 \end{aligned}
 \tag{4.3.5}$$

4.4 Results and discussions

We now use equations (4.3.4) and (4.3.5) to study the absorption-dispersion relation from two collective atoms without the inclusion of dipole-dipole interaction and driven by a detuned laser. From both equations, we find that absorption and dispersion spectra vanish for zero detuning. This agrees with Cordes et al. [4.6]. When a fixed strong coherent field is applied (e.g. $\frac{\Omega}{\gamma} = 40$) with finite detuning, we find that all spectra are asymmetric as expected. Essentially, we get absorption at $\omega = \omega_L + \alpha$ and amplification at $\omega = \omega_L - \alpha$ where $\alpha = \sqrt{4\Omega^2 + \Delta^2}$. The amplification and absorption can be explained systematically by using the dressed atomic states [4.11] (see figure 4.3.1). At $\omega = \omega_L$, the populations of the dressed states are equal, therefore there is no gain at the central atomic frequency (see figures 4.3.2-4.3.6). But the populations are different at $\omega \neq \omega_L$. Therefore, when $\omega = \omega_L + \alpha$, the probe that tuned to one of the Rabi sidebands would experience absorption. When $\omega = \omega_L - \alpha$, the probe tuned another Rabi sideband would experience amplification due to the population inversion between the dressed states [4.12]. Increasing the detuning gradually to larger values (say from $\frac{\Delta}{\gamma} = 10$ to $\frac{\Delta}{\gamma} = 40$) as in figures 4.3.2-4.3.5, the amplification is essentially unchanged but on the other hand absorption gradually increases. We observe that the absorption lineshape is Lorentzian. Note that results for $\frac{\Delta}{\gamma} \geq 50$ (see figure 4.3.6) are similar to those as exhibited in figures 4.3.2-4.3.5. To

confirm these analytical spectrum, we have plotted the corresponding numerical ones - see figure 4.3.7. Our numerical result is calculated by using a density matrix method as done for example in [4.13]. We observe that the magnitudes of maximum absorption and amplification are comparatively bigger than the corresponding analytical ones. Also, there is a dispersive profile at the central frequency for the numerical result

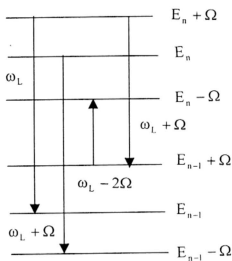


Figure 4.3.1 Energy levels of the dressed atomic states and transition process corresponding to unequal population when $\omega \neq \omega_L$.

which is not present for the analytical one. The dispersive profile from the numerical result is caused by the factor $\frac{1}{\Omega}$ which is ignored in the secular approximation technique. Nevertheless, in general both analytical and numerical results are in very good agreement.

We now study the corresponding dispersion spectrum from the two atoms driven by a strong detuned laser. Figure 4.3.8 shows a symmetrical dispersion spectrum which belongs to the Rayleigh-wing type (since $\frac{\Delta}{\gamma} = 0.1$). Note, however, that the refractive index does not vanish at the central frequency. This is also for other values of $\frac{\Delta}{\gamma} \neq 0$ in figures 4.3.9-4.3.12. As detuning gradually increases, we find that the maximum magnitudes of the dispersions also change. We obtained significant dispersions on both sides of the central frequency. Figure 4.3.13 is just to show $\frac{\Delta}{\gamma} \geq 50$ would produce similar results as for $\frac{\Delta}{\gamma} = 40$. We also plot the corresponding numerical dispersion in figure 4.3.14. Again the numerical dispersion spectrum is slightly different compared to the analytical one and a non-zero dip exists at the central frequency which is washed out in the analytical results. Again, a non-zero dip exists in the numerical result due to the factor $\frac{1}{\Omega}$ which is ignored in the secular approximation technique. Otherwise, in general both analytical and numerical results are in very good agreement.

In figures 4.3.15-4.3.19, we plot the analytical absorption-dispersion spectra. Clearly for finite detunings we do not find any large refractive index accompanied by vanishing absorption at the side bands. This is confirmed by the numerical result in figure 4.3.20. However, interestingly both analytical and numerical results show that we can get finite dispersion accompanied by zero absorption at the central frequency

of the spectrum. In figure 4.3.21 we plot the numerical result when $\frac{\Delta}{\gamma} = 0$ and $\frac{\Omega}{\gamma} = 40$. Clearly, we can conclude that finite dispersion accompanied by zero absorption at the Rabi sidebands is a feature unique for the collective atomic system driven by a strong detuned laser.

References:

- [4.1] G.S.Agarwal, L.M.Narducci, D.H.Feng and R.Gilmore, *Phys.Rev.Lett* **42** 260 (1979)
- [4.2] S.Ya.Kilin, *Sov.Phys. JETP* **51** 1081 (1980).
- [4.3] S.S.Hassan, G.P.Hilderred, R.R.Puri and S.V.Lawande, *J.Phys.B:At.Mol.Phys.* **15** 1029 (1982)
- [4.4] J.G.Cordes, *J.Phys.B:At.Mol.Phys.* **15** 4349 (1982)
- [4.5] J.G. Cordes, and J A Chevary, *J.Phys.B:At.Mol.Phys.* **17** 1913 (1984a)
- [4.6] J.G. Cordes, and J A Chevary, *J.Phys.B:At.Mol.Phys.* **17** 4163 (1984)
- [4.7] S.V.Lawande, B.N.Jagatap and R.R Puri, *J.Phys.B:At.Mol.Phys.* **18** 1711 (1985)
- [4.8] J.G.Cordes, *J.Phys.B:At.Mol.Phys.* **20** 1433 (1987)
- [4.9] M.Lax, *Phys.Rev.* **172**, 350 (1968)
- [4.10] B.R.Mollow , *Phys.Rev.A* **5**, 1522 (1972)
- [4.11] H.S.Freedhoff, *Phys.Rev.A* **19**, 132 (1979)
- [4.12] Z.Ficek, W.S.Smyth and S.Swain, *Optics Communications* **110**, 555 (1994)
- [4.13] M.R.B.Wahiddin, Ph.D Thesis, University of Manchester (1989)

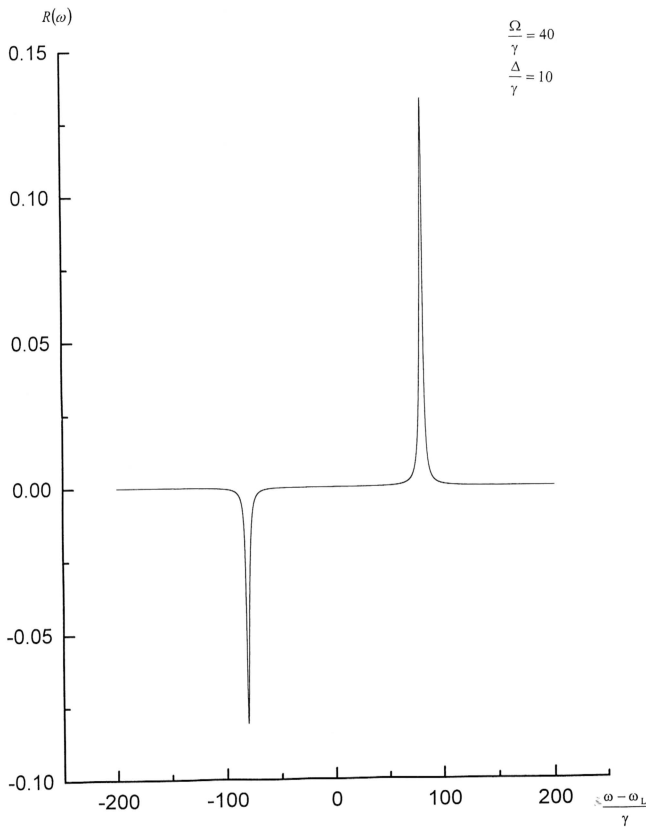


Figure 4.3.2 Plot of approximate absorption spectrum for two collective atoms driven by a detuned laser

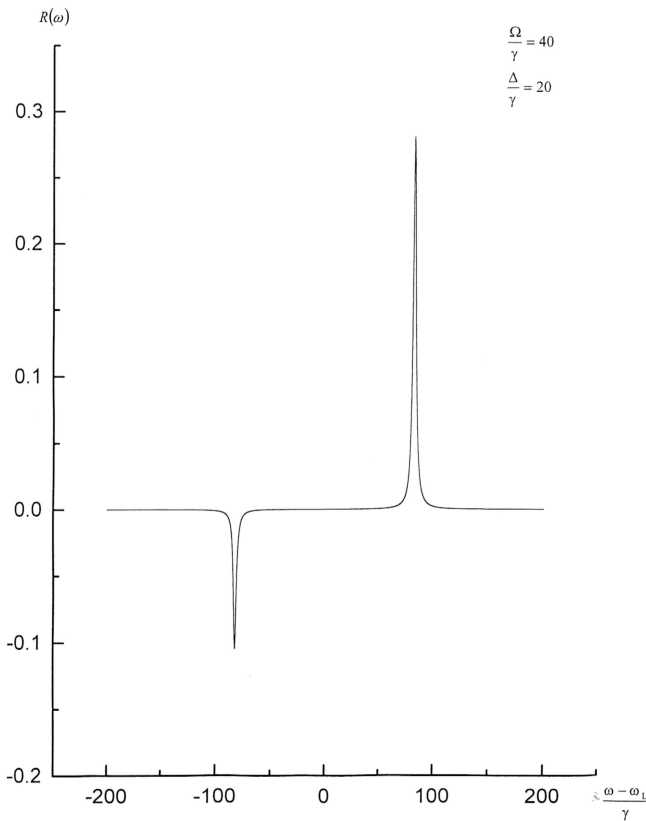


Figure 4.3.3 Plot of approximate absorption spectrum for two collective atoms driven by a detuned laser

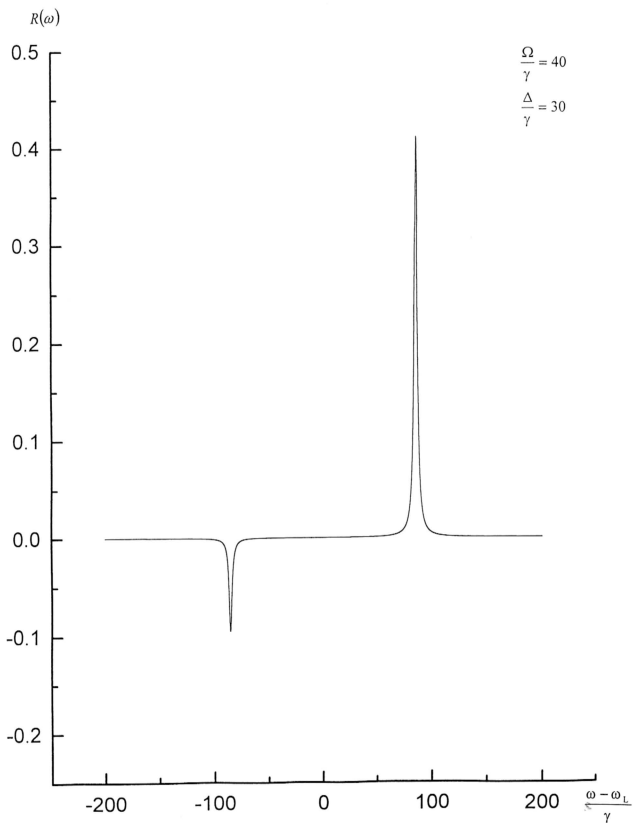


Figure 4.3.4 Plot of approximate absorption spectrum for two collective atoms driven by a detuned laser

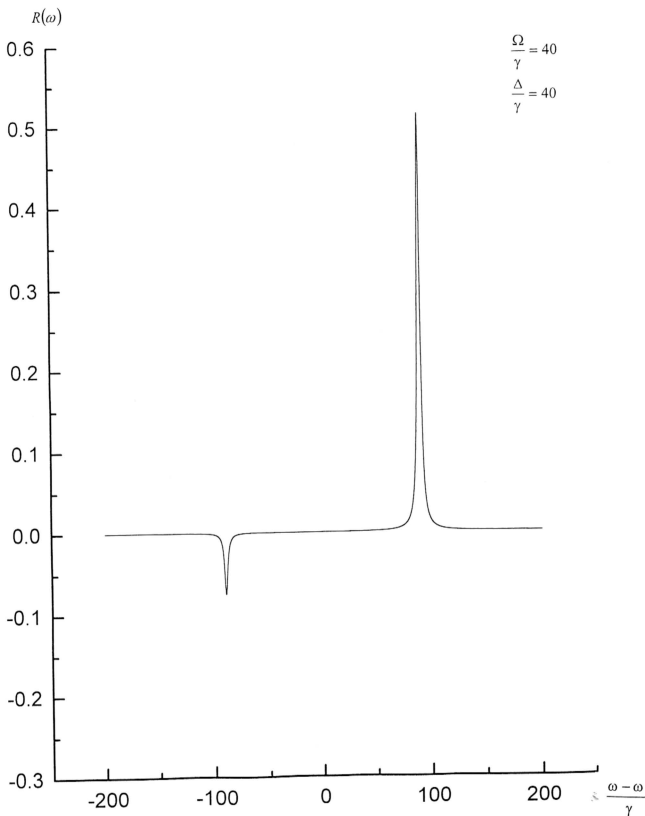


Figure 4.3.5 Plot of approximate absorption spectrum for two collective atoms driven by a detuned laser

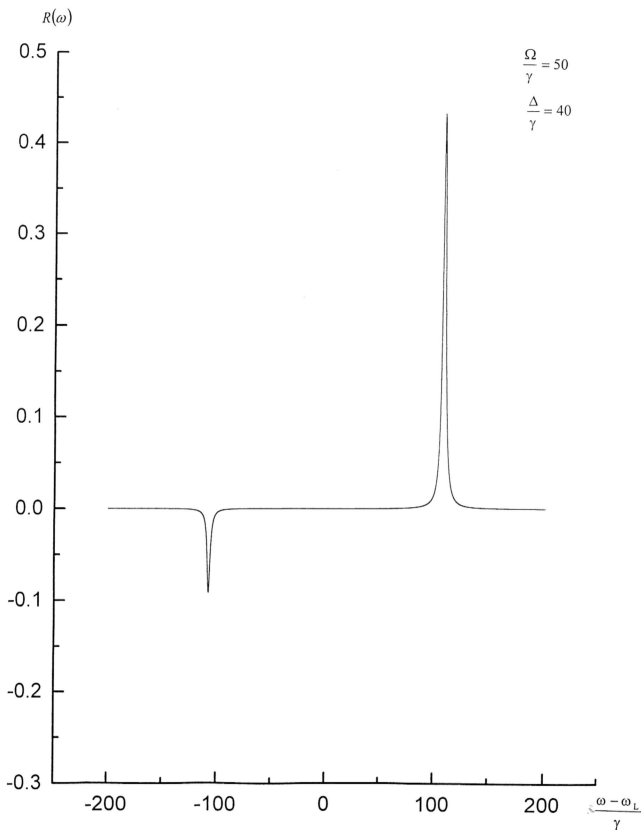


Figure 4.3.6 Plot of approximate absorption spectrum for two collective atoms driven by a detuned laser

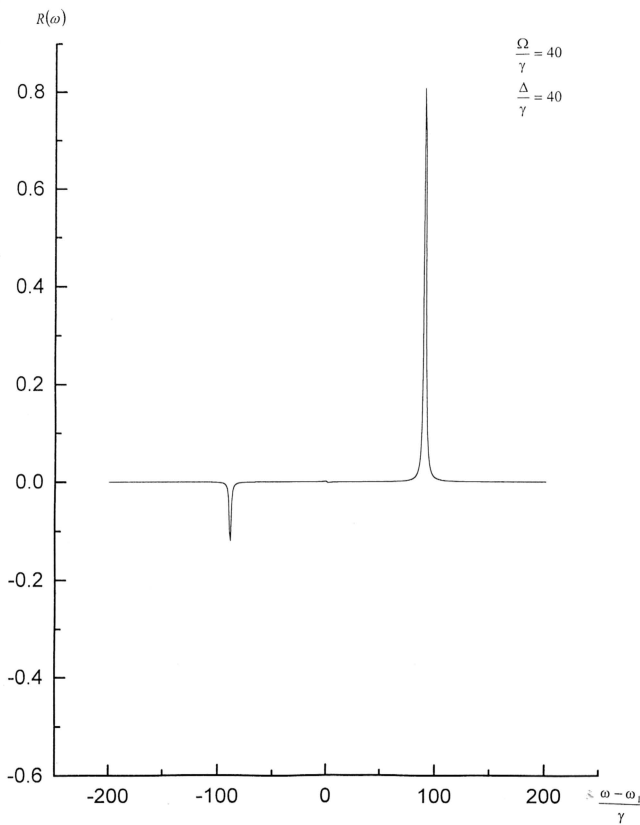


Figure 4.3.7 Plot of numerical absorption spectrum for two collective atoms driven by a detuned laser

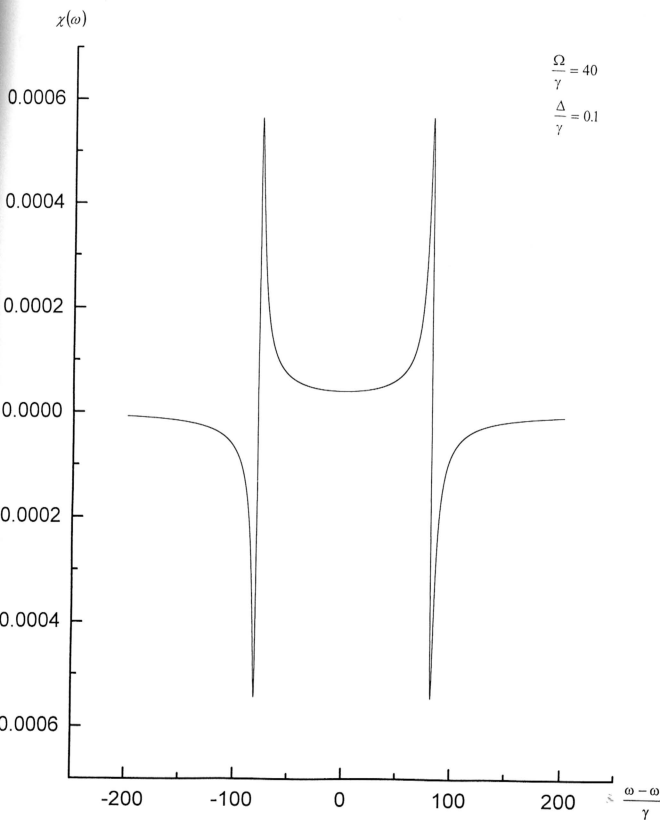


Figure 4.3.8 Plot of approximate dispersion spectrum for two collective atoms driven by a detuned laser

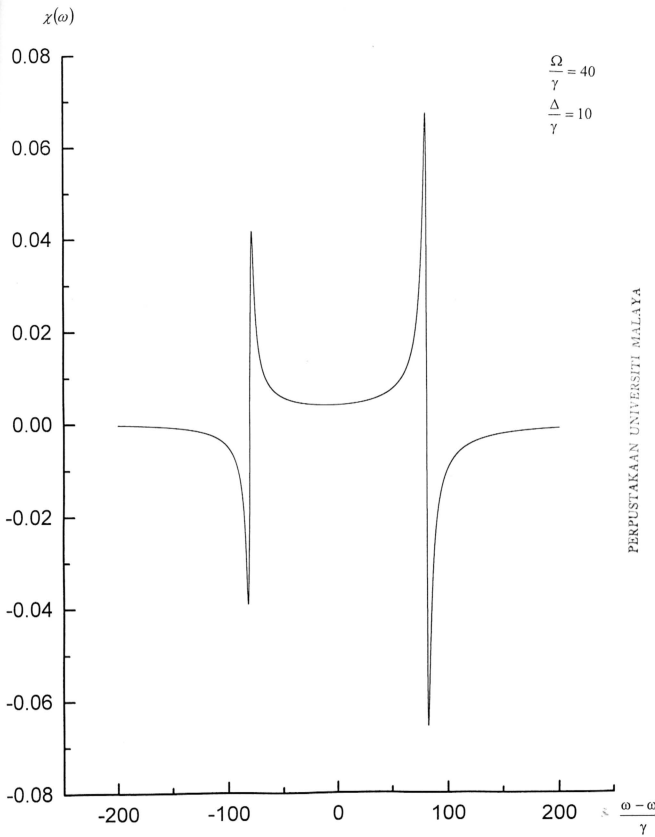


Figure 4.3.9 Plot of approximate dispersion spectrum for two collective atoms driven by a detuned laser

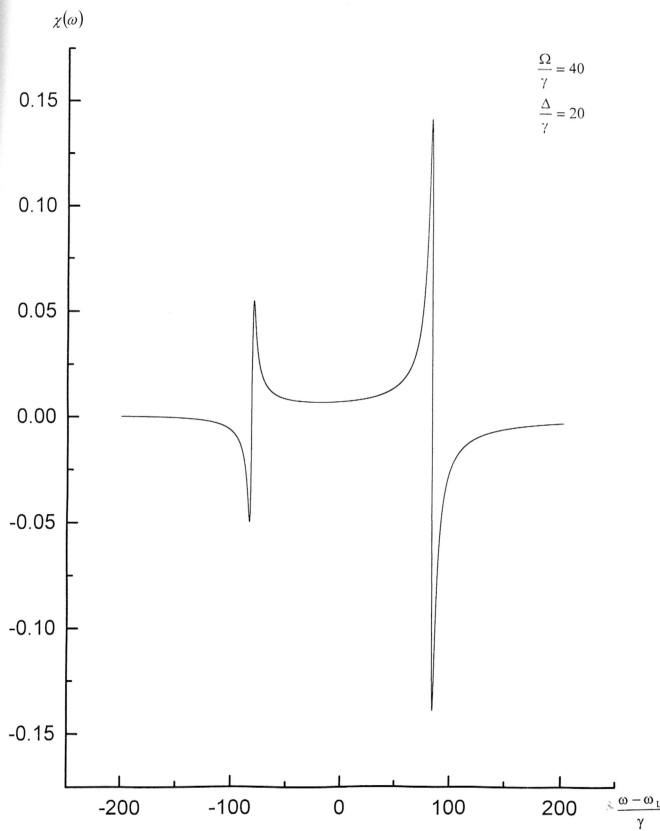


Figure 4.3.10 Plot of approximate dispersion spectrum for two collective atoms driven by a detuned laser

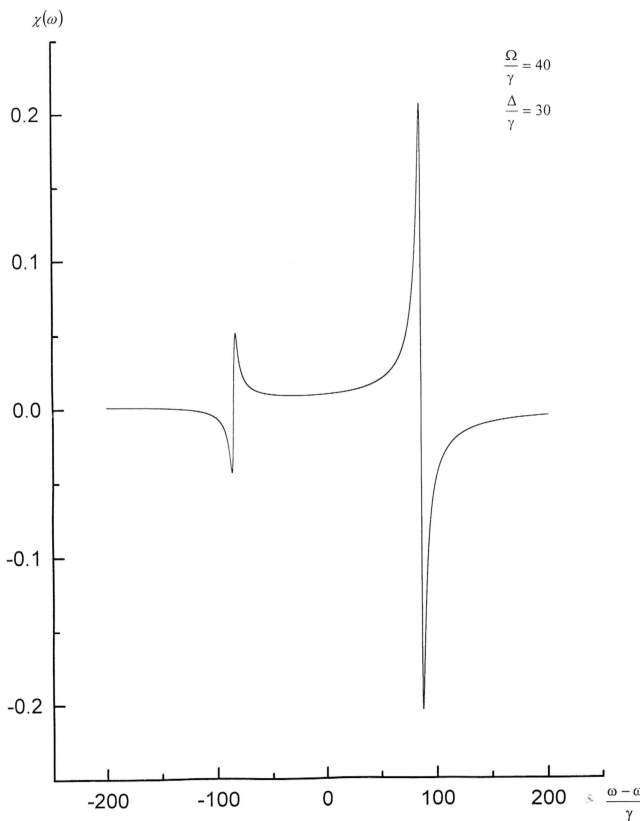


Figure 4.3.11 Plot of approximate dispersion spectrum for two collective atoms driven by a detuned laser

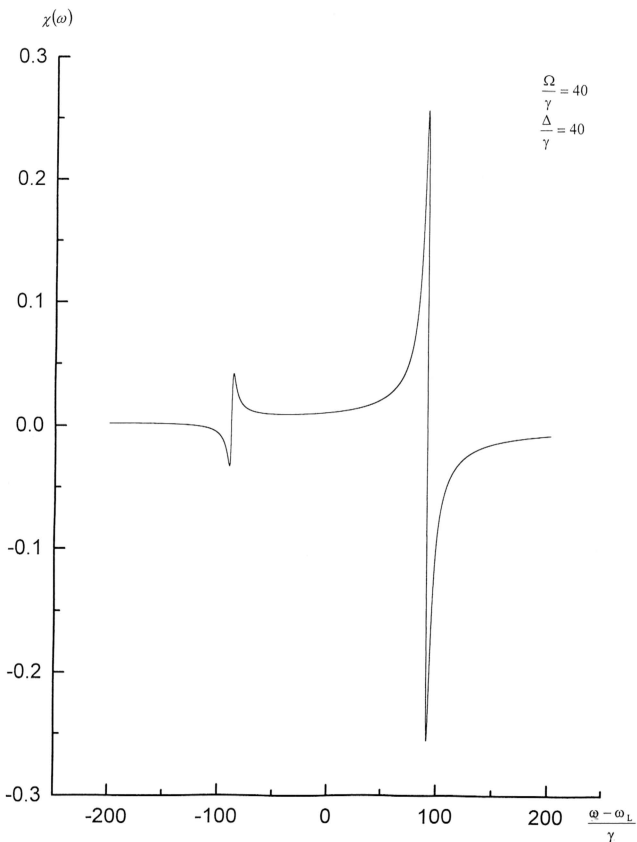


Figure 4.3.12 Plot of approximate dispersion spectrum for two collective atoms driven by a detuned laser

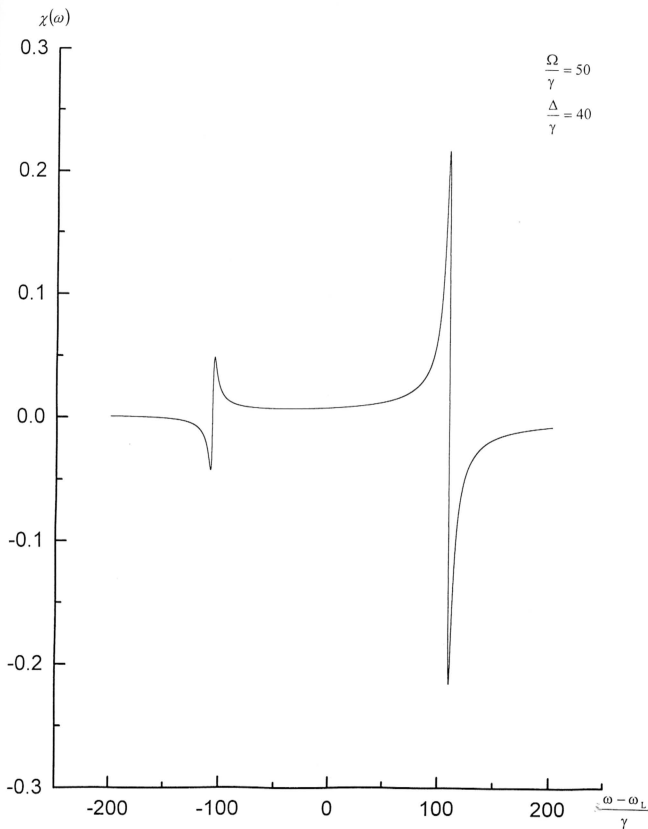


Figure 4.3.13 Plot of approximate dispersion spectrum for two collective atoms driven by a detuned laser

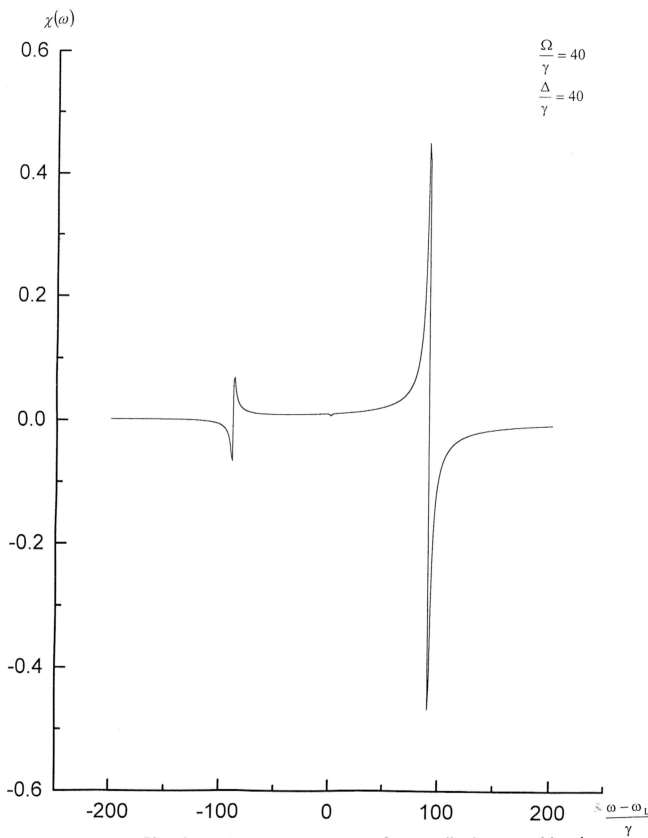


Figure 4.3.14 Plot of numerical dispersion spectrum for two collective atoms driven by a detuned laser

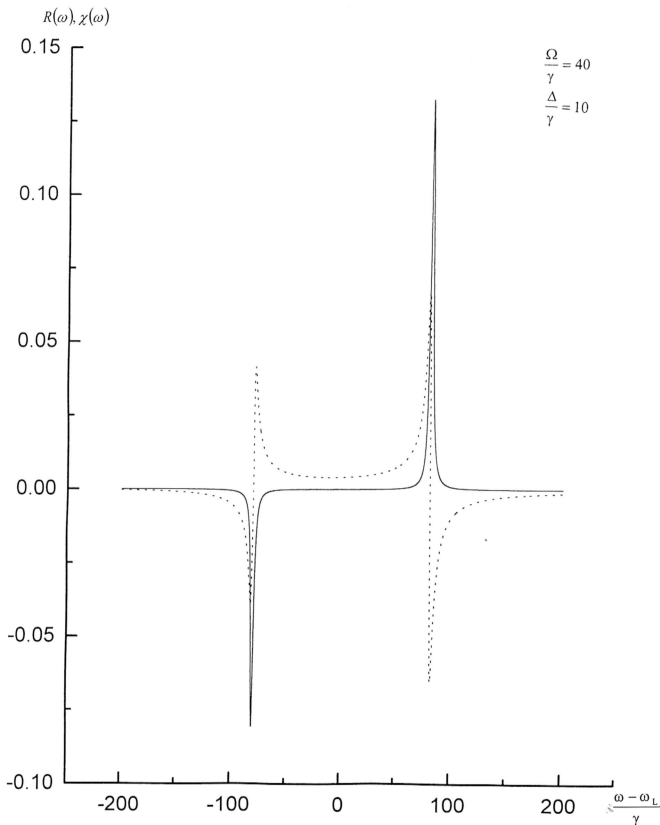


Figure 4.3.15 Plot of approximate absorption-dispersion spectrum for two collective atoms driven by a detuned laser. The solid and dashed lines represent the absorption and dispersion spectrum respectively.

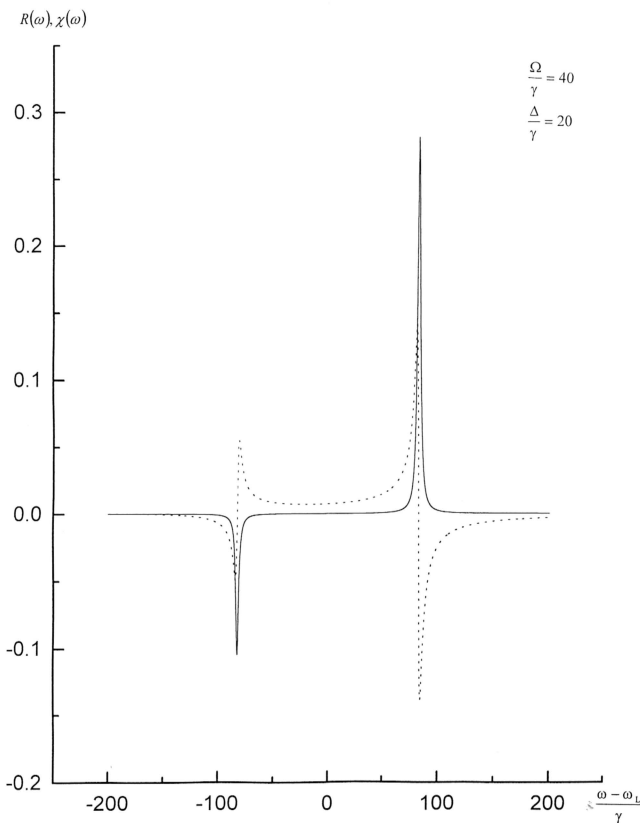


Figure 4.3.16 Plot of approximate absorption-dispersion spectrum for two collective atoms driven by a detuned laser. The solid and dashed lines represent the absorption and dispersion spectrum respectively.

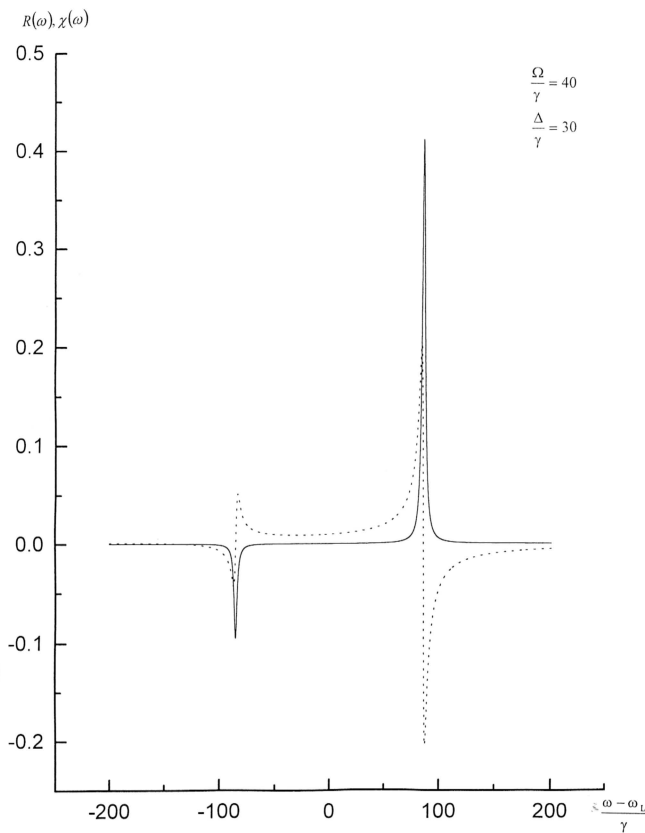


Figure 4.3.17 Plot of approximate absorption-dispersion spectrum for two collective atoms driven by a detuned laser. The solid and dashed lines represent the absorption and dispersion spectrum respectively.

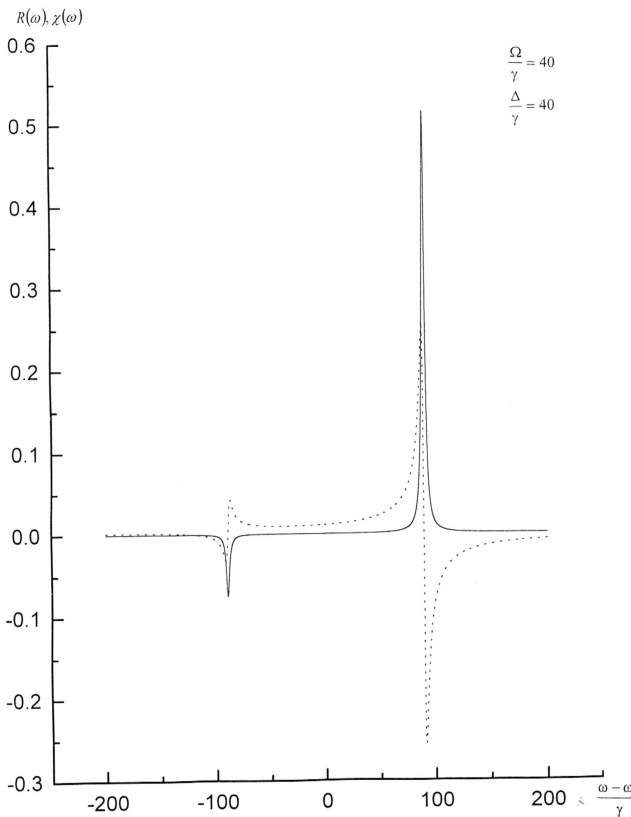


Figure 4.3.18 Plot of approximate absorption-dispersion spectrum for two collective atoms driven by a detuned laser. The solid and dashed lines represent the absorption and dispersion spectrum respectively.

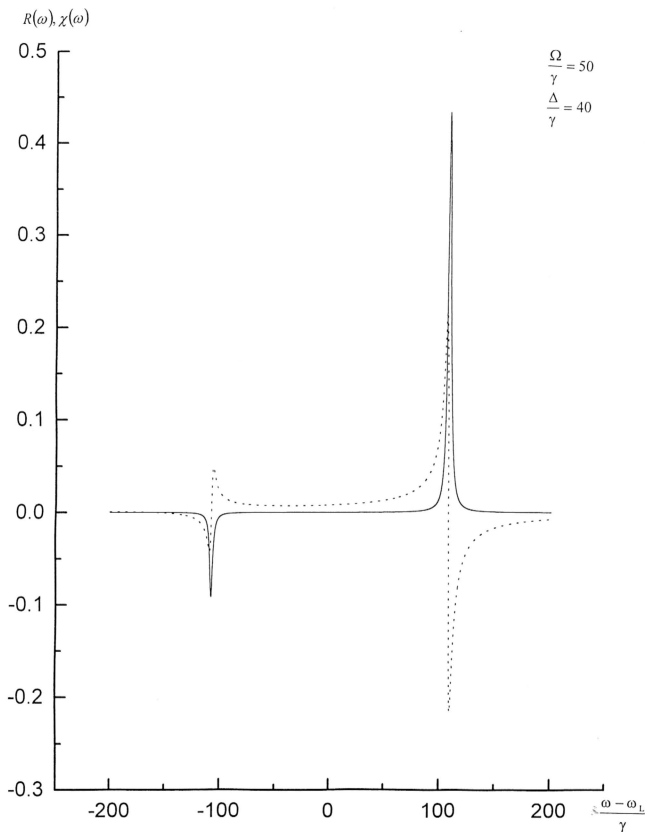


Figure 4.3.19 Plot of approximate absorption-dispersion spectrum for two collective atoms driven by a detuned laser. The solid and dashed lines represent the absorption and dispersion spectrum respectively.

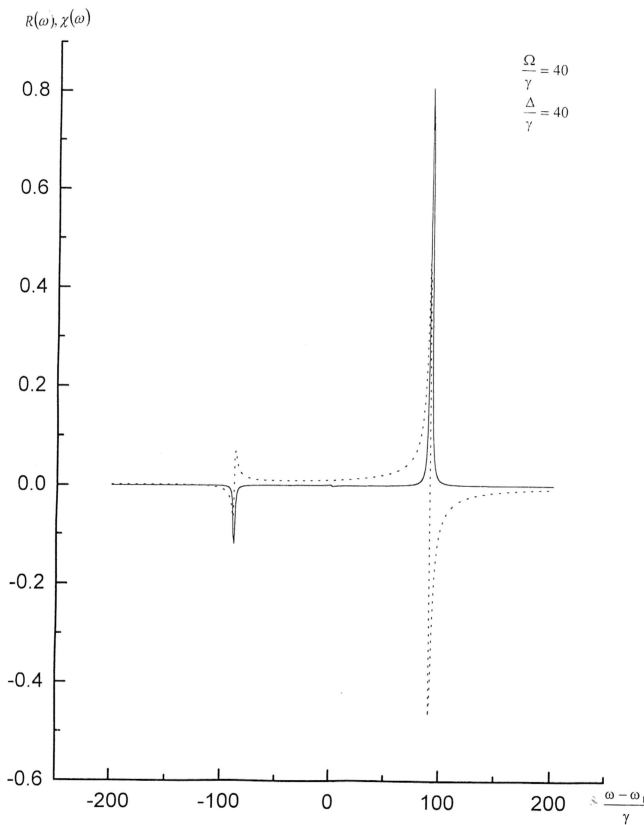


Figure 4.3.20 Plot of numerical absorption-dispersion spectrum for two collective atoms driven by a detuned laser. The solid and dashed lines represent the absorption and dispersion spectrum respectively.

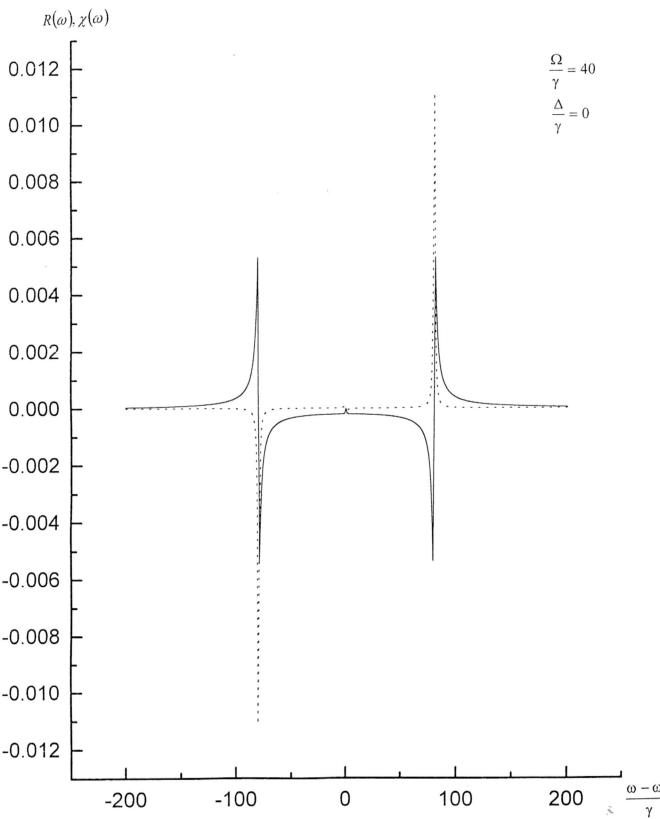


Figure 4.3.21 Plot of numerical absorption-dispersion spectrum for two collective atoms driven by a resonant laser. The solid and dashed lines represent the absorption and dispersion spectrum respectively.